IET Control Theory & Applications

Research Article

IET Journals
The Institution of Engineering and Technology

Trajectory tracking for wheeled mobile robots via model predictive control with softening constraints

ISSN 1751-8644
Received on 13th April 2017
Revised 24th September 2017
Accepted on 16th October 2017
E-First on 16th November 2017
doi: 10.1049/iet-cta.2017.0395
www.ietdl.org

Hongjiu Yang[1] ✉, Mingchao Guo[1], Yuanqing Xia[2], Lei Cheng[1]

[1]*Institute of Electrical Engineering, Yanshan University, Qinhuangdao 066004, People's Republic of China*
[2]*School of Automation, Beijing Institute of Technology, Beijing 100081, People's Republic of China*
✉ *E-mail: yanghongjiu@ysu.edu.cn*

Abstract: In this study, model predictive control with softening constraints is applied to a non-holonomic wheeled mobile robot for trajectory tracking in the presence of external disturbances. In order to improve real-time robustness of the wheeled mobile robot, a linearised tracking error model is used to predict system behaviours. The proposed control scheme contains a feedforward controller and a feedback controller, in which both control constraints and control increment constraints are considered to achieve trajectory tracking smoothly. Finally, numerical simulations demonstrate the performances of the control scheme.

1 Introduction

In recent decades, wheeled mobile robots (WMRs) have attracted considerable interest in robotics research owing to its extensive application in many fields [1, 2]. From the perspective of control, a WMR is usually formulated into a non-holonomic system. According to Brockett's necessary condition, the non-holonomic system cannot be asymptotically stabilised around an equilibrium point using smooth time-invariant feedback controllers [3]. In order to achieve posture stabilisation and trajectory tracking, many control methods have been proposed for the non-holonomic WMRs, such as smooth time-varying controller [4], discontinuous controller [5] and hybrid controller [6]. A vector field feedback control approach has been proposed for the WMR to achieve posture stabilisation and trajectory tracking in [7]. Backstepping techniques have been considered in designing tracking control strategies for WMR in [4]. A sliding-mode controller based on kinematic model of the WMR has been developed to track arbitrary trajectories even in large initial errors in [8]. A robust adaptive formation controller has been proposed for electrically driven non-holonomic WMR to achieve desired formation tracking and collision avoidance with static and moving obstacles in [9]. A robust controller based on an extended state observer has been proposed in [10], where the controller is aimed to achieve trajectory tracking of the WMR with unknown disturbances. A robust and adaptive control scheme has been presented using the finite-time algorithm in which a disturbance observer and an adaptive compensator are designed to cooperate with a tracking controller [11]. A hierarchical sliding-mode under-actuated controller has been designed for trajectory tracking of a mobile robot with frictions and uncertainties in [12]. An adaptive tracking control scheme has been presented for an asymmetrically actuated WMR with slipping/skidding dynamics and uncertain/unknown mass centre in [13]. A robust tracking control scheme has been proposed for WMRs with skidding, slipping and input disturbance in [14]. Furthermore, some control approaches have also been proposed based on intelligent control schemes, such as fuzzy logic control [15] and neural-network control [16]. In addition, most works above have not addressed the internal constraints yet and those methods require a post-processing step to scale the calculated control signals to their physical bounds. Hence, it has become a practically motivated and exciting scientific challenge to search for proper controllers to guarantee acceptable performance quality for the non-holonomic WMR with internal constraints.

In the last two decades, optional control was widely used in many fields [17, 18]. Model predictive control (MPC) is an important branch of optional control due to its applicability to non-linear multiple-input multiple-output systems with constraints and uncertainties [19, 20]. In the MPC, an optimal control input sequence is computed by solving a finite-horizon constrained optimisation problem. Only the first element of the optimal control input sequence is applied to plants. This process is repeated using updated measurements and a shifted horizon at the next sampling time [21]. According to the difference of prediction models, the MPC is divided into linear MPC and non-linear MPC. The non-linear MPC has been well developed [22]. A receding horizon controller has been developed for tracking control of a WMR in [23], where a terminal cost is constructed on a terminal region for the WMR. A robot formation algorithm based on non-linear MPC has been presented in [24], in which a suboptimal stable solution is used to reduce computational time. However, the computational effort is much larger than the linear MPC [25]. In the non-linear MPC, there exists a non-linear programming non-convex problem and a large number of decision variables to be solved online. Moreover, a global minimum of a cost function is in general impossible to obtain. Therefore, the linear MPC has been suggested as a suitable solution for motion control of mobile robots. The tracking-error kinematic model for WMR has been linearised at the equilibrium point and customised to an exact discrete-time form including time delays in [26]. A linear MPC scheme with friction compensation was proposed to solve the trajectory tracking problem for a three-wheeled omnidirectional mobile robot [27]. Tracking control via approximate linearisation using Taylor expansion for WMR error system has been proposed in [28]. However, most of control laws did not consider the constraints on control increments and external disturbances in the cost function. Hence, inspired by the authors [23, 24, 26–30], it is of great worth to design a trajectory tracking control law for the WMR with the constraints on control increments and external disturbances via the MPC method, which provides a motive to make an effort in this paper.

In this work, a kinematic error model of the non-holonomic WMR is linearised using Taylor expansion with remaining the high-order term. Then a control scheme with a combination of a feedforward control law and a feedback control law is designed. The feedforward controller is obtained from the given signal and the backward controller is derived from the optimal solution of MPC with actuator softening constraints. Furthermore, theoretical analysis of stability for the WMR system is given to the proposed

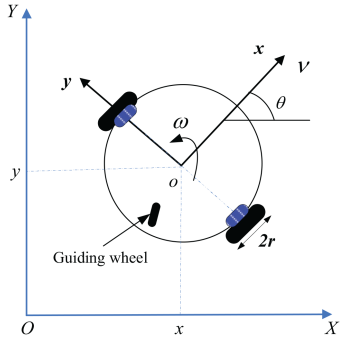

Fig. 1 *Non-holonomic WMR*

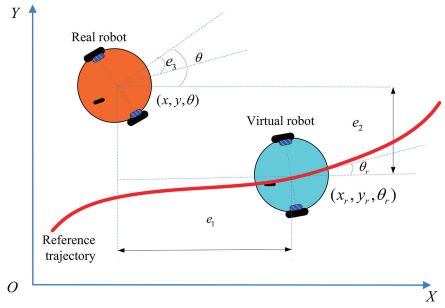

Fig. 2 *Trajectory tracking error*

MPC method. Finally, numerical simulations are shown to illustrate that the MPC scheme has an effective performance on tracking reference trajectories. The main contributions of this paper are summarised as below:

i. Both external disturbances and the high-order linearisation term are considered in a kinematic model.
ii. A control scheme is designed with a combination of a feedforward controller and a feedback controller.
iii. Control increment constraints and a relaxing factor avoid control jump and infeasible solutions, respectively.

Notations: In this paper, the superscript T stands for the transpose of a matrix. h represents the sampling time of simulation. $\mathbb{R}^n$ and $\mathbb{R}^n \times \mathbb{R}^n$ denote the n-dimensional Euclidean space and the set of all $n \times n$ real matrices, respectively. The operator $\bigoplus$ denotes Minkowski sum. n is the dimension of state variables and m is the dimension of control inputs. The shorthand diag$\{\cdots\}$ denotes a block diagonal matrix. $\|\cdot\|$ stands for Euclidean norm. $I_{n\times n}$ denotes an $n \times n$-dimensional unit matrix.

2 Non-holonomic WMR model

In this section, a non-holonomic WMR model is described. Then a corresponding discrete-time error model is presented so that a controller is designed to drive the WMR. A WMR's architecture with a guiding wheel is shown in Fig. 1. In Fig. 1, $\{O, X, Y\}$ is a global coordinate frame attached to the ground and $\{o, x, y\}$ is a local coordinate frame attached to the WMR. The distance between the two wheels is $2L$ and the diameter of the drive wheel is $2r$. Note that the WMR is pure rolling and cannot slip in a lateral direction, which implies a low speed during navigation [31]. As shown in [32], a kinematic model for the WMR under the non-integrable constraint is expressed as follows:

$$N(q(t))\dot{q}(t) = \dot{x}(t)\sin(\theta(t)) - \dot{y}(t)\cos(\theta(t))$$

where $N(q(t))$ is a constraint matrix defined over the global coordinates $q(t) = [x(t)\, y(t)\, \theta(t)]^{\mathrm{T}} \in \mathbb{R}^n$, $q(t)$ denotes the position and orientation of the WMR.

Let $S(q(t))$ be a full rank matrix formed by a linear combination of a vector field that spans the null space of the matrix $N(q(t))$. Consider the external disturbances caused by wind effects, road crown and superelevation [33], the first-order kinematic model of the WMR is formulated as

$$\dot{q}(t) = S(q(t))\begin{bmatrix}\nu(t)\\ \omega(t)\end{bmatrix} = \begin{bmatrix}\cos(\theta(t)) & 0\\ \sin(\theta(t)) & 0\\ 0 & 1\end{bmatrix} u(t) + \epsilon(t) \tag{1}$$

where $u(t) = [\nu(t)\, \omega(t)]^{\mathrm{T}} \in \mathbb{R}^m$ is a control input vector of the linear velocity and the angular velocity, $\epsilon(t)$ is the total external disturbance that is bounded. The left velocity and the right velocity of the WMR's wheels are given by $\nu_L(t) = \nu(t) - \omega(t)L/2$ and $\nu_R(t) = \nu(t) + \omega(t)L/2$, respectively.

The kinematic model (1) is rewritten in a compact form as follows:

$$\dot{q}(t) = f(q(t), u(t)) + \epsilon(t) \tag{2}$$

Furthermore, a virtual robot without disturbance is described as

$$\dot{q}_r(t) = f(q_r(t), u_r(t)) \tag{3}$$

Equation (2) is expanded in Taylor series around the reference point $(q_r(t), u_r(t))$. One has that

$$\begin{aligned}\dot{q}(t) = f(q_r(t), u_r(t)) &+ \left.\frac{\partial f(q(t), u(t))}{\partial q(t)}\right|_{q(t)=q_r(t),\, u(t)=u_r(t)}\\ &\times (q(t) - q_r(t)) + \left.\frac{\partial f(q(t), u(t))}{\partial u(t)}\right|_{q(t)=q_r(t),\, u(t)=u_r(t)}\\ &\times (u(t) - u_r(t)) + \zeta(t)\end{aligned} \tag{4}$$

where $\zeta(t) = \delta(q(t), u(t)) + \epsilon(t)$, $\delta(q(t), u(t))$ is a high-order term. It is obvious that $\zeta(t)$ is still bounded. Then (4) is shown in a simplified form as

$$\begin{aligned}\dot{q}(t) = f(q_r(t), u_r(t)) + f(q_r(t))(q(t) - q_r(t))\\ + f(u_r(t))(u(t) - u_r(t)) + \zeta(t)\end{aligned} \tag{5}$$

where $f(q_r(t))$ and $f(u_r(t))$ are the jacobian matrices of $f(q(t), u(t))$ with respect to $q(t)$ and $u(t)$ in the reference point $(q_r(t), u_r(t))$, respectively.

When the WMR is controlled to track a reference trajectory, there exist inevitably trajectory tracking errors. The trajectory tracking error $e(t) = [e_1(t)\, e_2(t)\, e_3(t)]^{\mathrm{T}}$ is expressed in the global frame, as shown in Fig. 2.

Let

$$\tilde{u}(t) = u(t) - u_r(t), \quad e(t) = q(t) - q_r(t) \tag{6}$$

By substituting (3) into (5), the error model of the WMR is shown as

$$\dot{e}(t) = A_e(t)e(t) + B_e(t)\tilde{u}(t) + \zeta(t) \tag{7}$$

where

$$A_e(t) = \begin{bmatrix}0 & 0 & -\nu_r(t)\sin(\theta_r(t))\\ 0 & 0 & \nu_r(t)\cos(\theta_r(t))\\ 0 & 0 & 0\end{bmatrix},$$

$$B_e(t) = \begin{bmatrix}\cos(\theta_r(t)) & 0\\ \sin(\theta_r(t)) & 0\\ 0 & 1\end{bmatrix}$$

The controllable matrix is $[B_e(t)\ A_e(t)B_e(t)\ A_e^2(t)B_e(t)]$. It is relatively easy to show that the matrix has full rank if $u_r(t)$ is non-zero. It implies that the WMR is controllable through the approximate linearisation of the WMR model (1). According to Brockett's condition [3], it is possible to achieve trajectory tacking for the WMR model (1) with a time-varying feedback controller.

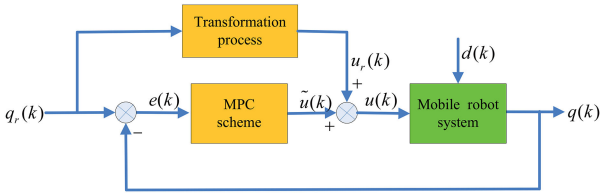

Fig. 3 *Control structure of the system*

In order to track a reference trajectory, the error model (7) is transformed into a discrete-time form using the approximately discrete method. The discrete-time error model (7) is rewritten as follows:

$$e(k+1) = A(k)e(k) + B(k)\tilde{u}(k) + d(k) \tag{8}$$

The discrete matrices $A(k)$ and $B(k)$ are derived by $A(k) = I_{n\times n} + A_e(k)h$ and $B(k) = B_e(k)h$, i.e.

$$A(k) = \begin{bmatrix} 1 & 0 & -\nu_r(k)\sin(\theta_r(k))h \\ 0 & 1 & \nu_r(k)\cos(\theta_r(k))h \\ 0 & 0 & 1 \end{bmatrix},$$
$$B(k) = \begin{bmatrix} \cos(\theta_r(k))h & 0 \\ \sin(\theta_r(k))h & 0 \\ 0 & h \end{bmatrix}, \quad d(k) = \zeta(k)h$$

Remark 1: It is inevitable that digital realisation of control systems needs discretisation. The discretisation is obtained either via a controller or a system, and the latter is chosen in this paper. The accurate discretisation [34] and approximately discretisation [35] are widely used method for its simplicity. When the sampling time h is sufficiently small for the approximately discretisation, the error of the approximately discretisation can be ignored.

3 Design of the controller

According to (6), the controller of the WMR is designed in discretisation form as

$$u(k) = u_r(k) + \tilde{u}(k) \tag{9}$$

where $u_r(k)$ and $\tilde{u}(k)$ are feedforward controller and feedback controller at time instant k. The control structure is shown in Fig. 3.

In Fig. 3, the transformation process and the MPC scheme are feedforward and feedback progress, respectively. The external disturbances $d(k)$ are applied to the WMR system (1). The solution of (9) with a combination of the feedforward controller and the feedback controller is shown as the following subsection.

3.1 Feedforward control

For a given reference trajectory $(x_r(t), y_r(t))$, $t \in [(k-1)h, kh]$, the feedforward control input $u_r(k) = [\nu_r(k)\ \omega_r(k)]^{\mathrm{T}}$ is derived. The feedforward control input $u_r(k)$ drives the WMR system (1) along a reference trajectory only if there are neither disturbances nor initial state errors. When the robot tracks a desired trajectory, the linear velocity $\nu_r(k)$ is calculated as follows:

$$\nu_r(k) = \pm\frac{\sqrt{(x_r(k)-x_r(k-1))^2 + (y_r(k)-y_r(k-1))^2}}{h} \tag{10}$$

When the robot runs forward, (10) is positive, and vice versa. The tangent angle of each sampling instant k on the reference trajectory is given as

$$\theta_r(k) = \arctan\left(\frac{y_r(k)-y_r(k-1)}{x_r(k)-x_r(k-1)}\right) + \tau\pi \tag{11}$$

where τ stands for the desired drive direction with $\tau = 0$ for forward and $\tau = 1$ for reverse. The angular velocity $\omega_r(k)$ of virtual WMR is obtained as

$$\omega_r(k) = \frac{\theta_r(k) - \theta_r(k-1)}{h} \tag{12}$$

The control inputs $\nu_r(k)$ and $\omega_r(k)$ are obtained by the reference path and (10)–(12). That is, the feedforward control law $u_r(k)$ is derived.

3.2 MPC scheme

In this section, the feedback controller is designed so that the mobile robot is steered to a referenced trajectory based on the MPC method. From [35], a cost function with soft constraints is shown as

$$\begin{aligned} J(k) = \sum_{i=1}^{N_p} &[(\eta(k+i|k) - \eta_r(k+i|k))^T Q(\eta(k+i|k) \\ &-\eta_r(k+i|k))] + \sum_{i=0}^{N_c-1} [\Delta\tilde{u}^T(k+i|k)R \\ &\times \Delta\tilde{u}(k+i|k)] + \varepsilon(k)^T\rho\varepsilon(k) \end{aligned} \tag{13}$$

where $\eta(k+i|k)$ and $\eta_r(k+i|k)$ denote the output state and the reference output state in the predicted horizon, respectively, $\Delta\tilde{u}(k+i|k)$ denotes the control input increment of the error model (8) in the control horizon with $\Delta\tilde{u}(k+i|k) = \tilde{u}(k+i|k) - \tilde{u}(k+i-1|k)$, the predicted horizon is N_p and the control horizon is N_c. Note that $N_p \geq 1$ and $1 \leq N_c \leq N_p$, $\varepsilon(k) = [\varepsilon_1(k)\ \varepsilon_2(k)]^{\mathrm{T}}$ is the relaxing factor which prevents from emerging infeasible solutions during execution [36]. In the cost function (13), the first item on the right side describes the capability of trajectory tracking and the second item reflects the constraint on the change of the feedback control input. Q, R and ρ stand for weighting matrices, where $Q \in \mathbb{R}^n \times \mathbb{R}^n$ is positive semi-definite, both $R \in \mathbb{R}^m \times \mathbb{R}^m$ and $\rho \in \mathbb{R}^m \times \mathbb{R}^m$ are positive definite. The selection principle of weighting matrices, which guarantees stability of the closed-loop error system (8), has been shown in [37].

Remark 2: A summary of the available tuning guidelines for MPC scheme has been provided in [37]. The weighting parameters Q, R and ρ are set as diagonal matrices [23, 35]. The ratio of the diagonal elements in Q determines the sensitivity of the resulting controller to a certain error, i.e. $\eta(k+i|k) - \eta_r(k+i|k)$; the higher value of the diagonal elements increases, the more sensitivity to the corresponding error is. The diagonal elements in R define the energy of the control signal $\Delta\tilde{u}(k+i|k)$; the lower value of the elements is, the more energy-consuming control is. Similarly, the weighting matrix ρ is non-negative scalar relative to the relaxing factor $\varepsilon(k)$; the high value recovers the solution to the hard optimisation problem [36]. The predicted horizon N_p and the control horizon N_c influence the step size of iteration. The small values of N_p and N_c result in fast control response.

For any real world plant, control inputs are subject to physical limitations. Hence, the bounds on the control inputs are considered when control inputs are computed. Considering the relaxing factor at the same time, the control input is expressed as

$$\begin{aligned} \Omega_u \triangleq \{&\tilde{u}_{\min}(k) + \varepsilon_1(k)v_{1\min} \leq \tilde{u}(k) \\ &\leq \tilde{u}_{\max}(k) + \varepsilon_1(k)v_{1\max}\} \end{aligned} \tag{14}$$

In order to avoid the phenomenon of jump, the control increment constraints are shown as

$$\begin{aligned} \Omega_{\Delta u} \triangleq \{&\Delta\tilde{u}_{\min}(k) + \varepsilon_2(k)v_{2\min} \leq \Delta\tilde{u}(k) \\ &\leq \Delta\tilde{u}_{\max}(k) + \varepsilon_2(k)v_{2\max}\} \end{aligned} \tag{15}$$

where Ω_u and $\Omega_{\Delta u}$ are constraint sets corresponds to $\tilde{u}(k)$ and $\Delta\tilde{u}(k)$, respectively, $\tilde{u}_{\min}(k)$ and $\tilde{u}_{\max}(k)$ are the controller bounds, $\Delta\tilde{u}_{\min}(k)$ and $\Delta\tilde{u}_{\max}(k)$ are the control increment bounds, $v_{1\min}$ and $v_{2\min}$ are the lower bounds of the relaxing factor, $v_{1\max}$ and $v_{2\max}$ are the upper bounds. Therefore, the feedback controller is obtained by minimising the cost function (13) with the constraint sets Ω_u and $\Omega_{\Delta u}$. The key question is how to solve the cost function (13) with the constraint sets Ω_u and $\Omega_{\Delta u}$.

3.3 Design of cost function

In order to solve the cost function (13), a variable is given as

$$\xi(k|k) = \begin{bmatrix} e(k|k) \\ \tilde{u}(k-1|k) \end{bmatrix}$$

Then (8) is converted to state-space equations as follows:

$$\xi(k+1|k) = \tilde{A}(k)\xi(k|k) + \tilde{B}(k)\Delta\tilde{u}(k|k) + \tilde{d}(k|k) \tag{16}$$

$$\eta(k|k) = \tilde{C}\xi(k|k) \tag{17}$$

where

$$\tilde{A}(k) = \begin{bmatrix} A(k) & B(k) \\ 0_{m\times n} & I_m \end{bmatrix}, \quad \tilde{B}(k) = \begin{bmatrix} B(k) & I_m \end{bmatrix}^{\mathrm{T}},$$
$$\tilde{C} = \begin{bmatrix} I_{n\times n} & 0_{n\times m} \end{bmatrix}, \quad \tilde{d}(k|k) = \begin{bmatrix} d(k|k) & 0_{m\times 1} \end{bmatrix}^{\mathrm{T}},$$
$$\Delta\tilde{u}(k|k) = \tilde{u}(k|k) - \tilde{u}(k-1|k)$$

At the current time step k, the future states $\xi(k+i|k)$, $i = 1, 2, \ldots, N_p$ is iterated by (16). One has that

$$\begin{aligned}
\xi(k+1|k) &= \tilde{A}(k)\xi(k|k) + \tilde{B}(k)\Delta\tilde{u}(k|k) + \tilde{d}(k|k) \\
\xi(k+2|k) &= \tilde{A}(k+1)\xi(k+1|k) + \tilde{B}(k+1)\Delta\tilde{u}(k+1|k) \\
&\quad + \tilde{d}(k+1|k) \\
&= \tilde{A}(k+1)\tilde{A}(k)\xi(k|k) + \tilde{A}(k+1)\tilde{B}(k)\Delta\tilde{u}(k|k) \\
&\quad + \tilde{A}(k+1)\tilde{d}(k|k) + \tilde{B}(k+1)\Delta\tilde{u}(k+1|k) \\
&\quad + \tilde{d}(k+1|k) \\
&\vdots \\
\xi(k+N_p|k) &= \Lambda(N_p-1,0)\xi(k|k) + \sum_{j=1}^{N_c} \Lambda(N_p-1,i) \\
&\quad \times \tilde{B}(k+i-1)\Delta\tilde{u}(k+i-1|k) \\
&\quad + \sum_{j=1}^{N_p-1} \Lambda(N_p-1,i)\tilde{d}(k+i|k)
\end{aligned} \tag{18}$$

where

$$\Lambda(h,i) = \prod_{j=i}^{h} A(k+j)$$

By substituting (18) into (17), the predicted output expression of system (17) is obtained in a matrix form

$$Y(k) = M(k)\xi(k|k) + \Theta(k)\Delta U(k) + \Gamma(k)D(k)$$

where the predicted output expression $Y(k) \in \mathbb{R}^{nN_p}$ and matrix $M(k) \in \mathbb{R}^{nN_p} \times \mathbb{R}^{n+m}$ are obtained as follows:

$$Y(k) = \begin{bmatrix} \eta(k+1|k) \\ \eta(k+2|k) \\ \vdots \\ \eta(k+N_c|k) \\ \vdots \\ \eta(k+N_p|k) \end{bmatrix}, \quad M(k) = \begin{bmatrix} \tilde{C}\tilde{A}(k) \\ \tilde{C}\tilde{A}(k+1)\tilde{A}(k) \\ \vdots \\ \tilde{C}\Lambda(N_c-1,0) \\ \vdots \\ \tilde{C}\Lambda(N_p-1,0) \end{bmatrix}$$

The predicted control input increment $\Delta U(k) \in \mathbb{R}^{mN_c}$ and disturbance $D(k) \in \mathbb{R}^{(m+n)N_p}$ read

$$\Delta U(k) = \begin{bmatrix} \Delta\tilde{u}(k|k) \\ \Delta\tilde{u}(k+1|k) \\ \vdots \\ \Delta\tilde{u}(k+N_c-1|k) \end{bmatrix},$$
$$D(k) = \begin{bmatrix} \tilde{d}(k|k) \\ d(k+1|k) \\ \vdots \\ \tilde{d}(k+N_c-1|k) \\ \vdots \\ \tilde{d}(k+N_p-1|k) \end{bmatrix}$$

Moreover, matrices $\Gamma(k) \in \mathbb{R}^{nN_p} \times \mathbb{R}^{(m+n)N_p}$ and $\Theta(k) \in \mathbb{R}^{nN_p} \times \mathbb{R}^{mN_c}$ are given as follows:

$$\Gamma(k) = \begin{bmatrix} \tilde{C} & 0_{n\times(n+m)} & \cdots & 0_{n\times(n+m)} \\ \tilde{C}\tilde{A}(k+1) & \tilde{C} & \cdots & 0_{n\times(n+m)} \\ \vdots & \vdots & \ddots & \vdots \\ \tilde{C}\Lambda(N_p-1,1) & \tilde{C}\Lambda(N_p-1,2) & \cdots & \tilde{C} \end{bmatrix}$$

and

$$\Theta(k) = \begin{bmatrix} \tilde{C}\tilde{B}(k) & 0_{n\times(n+m)} & \cdots & 0_{n\times(n+m)} \\ \tilde{C}\tilde{A}(k+1)\tilde{B}(k) & \tilde{C}\tilde{B}(k+1) & \cdots & 0_{n\times(n+m)} \\ \vdots & \vdots & \ddots & \vdots \\ \tilde{C}\Lambda(N_c-1,1)\tilde{B}(k) & \tilde{C}\Lambda(N_c-1,2)\tilde{B}(k+1) & \cdots & \tilde{C}\tilde{B}(k+N_c-1) \\ \vdots & \vdots & \ddots & \vdots \\ \tilde{C}\Lambda(N_p-1,1)\tilde{B}(k) & \tilde{C}\Lambda(N_p-1,2)\tilde{B}(k+1) & \cdots & \tilde{C}\Lambda(N_p-1,N_c)\tilde{B}(k+N_c-1) \end{bmatrix}$$

Then the cost function (13) is rewritten as

$$J(k) = \tilde{Y}(k)^T\tilde{Q}\tilde{Y}(k) + \Delta U^T(k)\tilde{R}\Delta U(k) + \varepsilon^T\rho\varepsilon \tag{19}$$

where $\tilde{Q} = \bigoplus_{i=1}^{N_p} Q(i)$, $\tilde{R} = \bigoplus_{i=1}^{N_c-1} R(i)$. Note that $\tilde{Y}(k) = Y(k) - Y_r(k)$, $Y_r(k)$ is the future reference out signal. The reference output states are set to an exponential decline form as follows:

$$Y_r(k) = \begin{bmatrix} \tilde{C}\tilde{A}_r & \tilde{C}\tilde{A}_r^2 \cdots \tilde{C}\tilde{A}_r^{N_p} \end{bmatrix}\eta(k|k)$$

$Y_r(k) = 0$ is a special case at $\tilde{A}_r = 0$. It means that the actual trajectory under the controller precisely follows the reference trajectory without errors over the prediction horizon N_p.

Therefore, the cost function (19) is reformulated as

$$J(k)=\frac{1}{2}\begin{bmatrix}\Delta U(k)\\ \varepsilon(k)\end{bmatrix}^{\mathrm{T}}H(k)\begin{bmatrix}\Delta U(k)\\ \varepsilon(k)\end{bmatrix}+F(k)\begin{bmatrix}\Delta U(k)\\ \varepsilon(k)\end{bmatrix}+E(k)^{T}\tilde{Q}E(k) \tag{20}$$

where

$$H(k)=\begin{bmatrix}2(\Theta^{T}(k)\tilde{Q}\Theta(k)+\tilde{R}) & 0_{mN_c\times 2}\\ 0_{2\times mN_c} & 2\rho\end{bmatrix}$$

and $F=\begin{bmatrix}2E^{T}(k)\tilde{Q}\Theta(k) & 0_{1\times 2}\end{bmatrix}$, $E(k)=M(k)\xi(k)-Y_r(k)+\Gamma(k)D(k)$. The positive definite matrix H is a Hessian matrix that describes a quadratic part of the cost function (20), $F(k)$ describes the linear part, $E(k)$ is the tracking error in the predictive horizon, $E^{T}(k)\tilde{Q}E(k)$ is a matrix that is independent on $\Delta U(k)$ and the determination of (20). Therefore, the irrelative part $E^{T}(k)\tilde{Q}E(k)$ is omitted in the cost function (20).

3.4 Constraints of cost function

From the cost function (20), the variables to be solved are control increments $\Delta U(k)$. Then the constraint conditions (14) is transformed into a form of the control increments according to the relationship between $\tilde{u}(k)$ and $\Delta\tilde{u}(k)$, i.e.

$$\tilde{u}(k)=\tilde{u}(k-1)+\Delta\tilde{u}(k)$$

The constrains of (14) and (15) are transformed into a standard form as follows:

$$\begin{bmatrix}L_{\Delta u} & -V_{1\max} & 0_{mN_c\times 1}\\ -L_{\Delta u} & V_{1\min} & 0_{mN_c\times 1}\\ I_{\Delta u} & 0_{mN_c\times 1} & V_{2\max}\\ -I_{\Delta u} & 0_{mN_c\times 1} & V_{2\min}\end{bmatrix}\begin{bmatrix}\Delta U(k)\\ \tilde{\varepsilon}\end{bmatrix}\le\begin{bmatrix}U_{\max}-L_u\tilde{u}(k-1)\\ -U_{\min}+L_u\tilde{u}(k-1)\\ \Delta U_{\max}\\ -\Delta U_{\min}\end{bmatrix} \tag{21}$$

where

$$L_{\Delta u}=\begin{bmatrix}I & 0 & \cdots & 0\\ I & I & \cdots & 0\\ \vdots & \vdots & \ddots & \vdots\\ I & I & \cdots & I\end{bmatrix}\in\mathbb{R}^{mN_c}\times\mathbb{R}^{mN_c},$$

$$I_{\Delta u}=\begin{bmatrix}1 & 0 & \cdots & 0\\ 0 & 1 & \cdots & 0\\ \vdots & \vdots & \ddots & \vdots\\ 0 & 0 & \cdots & 1\end{bmatrix}\in\mathbb{R}^{mN_c}\times\mathbb{R}^{mN_c},$$

$$L_u=\begin{bmatrix}1\\ 1\\ \vdots\\ 1\end{bmatrix}\in\mathbb{R}^{mN_c},\quad V_{1\max}=\begin{bmatrix}v_{1\max}\\ v_{1\max}\\ \vdots\\ v_{1\max}\end{bmatrix}\in\mathbb{R}^{mN_c},$$

$$U_{\max}=\begin{bmatrix}u_{\max}\\ u_{\max}\\ \vdots\\ u_{\max}\end{bmatrix}\in\mathbb{R}^{mN_c}$$

Similar to $V_{1\max}$ and $U_{\max}$, the form of $V_{1\min}$, $V_{2\max}$, $V_{2\min}$ and $U_{\min}$ can also be derived. In addition, the constraints of relaxing factor and the external disturbances are

$$0_{2\times 1}\le\tilde{\varepsilon}(k)\le\alpha(k), \tag{22}$$

$$d_{\min}(k)\le d(k)\le d_{\max}(k) \tag{23}$$

where $\alpha(k)=\begin{bmatrix}\alpha_{1\max}(k)\,\alpha_{2\max}(k)\end{bmatrix}^{\mathrm{T}}$. Both $\alpha_{1\max}(k)$ and $\alpha_{2\max}(k)$ are two proper positives, $d_{\min}(k)$ and $d_{\max}(k)$ are the bounds of the disturbances.

Let

$$\Xi=\begin{bmatrix}L_{\Delta u} & -V_{1\max} & 0_{mN_c\times 1}\\ -L_{\Delta u} & V_{1\min} & 0_{mN_c\times 1}\\ I_{\Delta u} & 0_{mN_c\times 1} & V_{2\max}\\ -I_{\Delta u} & 0_{mN_c\times 1} & V_{2\min}\end{bmatrix},$$

$$\Upsilon(k)=\begin{bmatrix}U_{\max}-L_u\tilde{u}(k-1)\\ -U_{\min}+L_u\tilde{u}(k-1)\\ \Delta U_{\max}\\ -\Delta U_{\min}\end{bmatrix}$$

and $\varsigma(k)=[\Delta U(k)\,\varepsilon]^{\mathrm{T}}$. The cost function (20) with constrains (21)–(23) are rewritten as follows:

$$\min\ J(k)=\frac{1}{2}\varsigma(k)^{T}H\varsigma(k)+F\varsigma(k) \tag{24}$$

s.t.

$$\Xi\varsigma(k)\le\Upsilon(k) \tag{25}$$

By searching for the minimum of the cost function (24) with constraint (25), a series of feedback control input increments and relaxing factors in the control horizon N_c are shown as

$$[\Delta U^{*}(k)\varepsilon^{*}(k)]=[\Delta\tilde{u}^{*}(k)\Delta\tilde{u}^{*}(k+1)\cdots\Delta\tilde{u}^{*}(N_c-1)\varepsilon_1^{*}(k)\varepsilon_2^{*}(k)]^{\mathrm{T}} \tag{26}$$

Although the prediction and optimisation are performed over a control horizon, only the first element of the control sequences (26) at the time instant k is applied to system, i.e.

$$\tilde{u}^{*}(k)=\tilde{u}(k-1)+\Delta\tilde{u}^{*}(k)$$

Then the proposed control scheme is obtained as

$$u^{*}(k)=u_r(k)+\tilde{u}^{*}(k) \tag{27}$$

At the next clock tick, the above procedure is repeated again. Because the control sequences (26) has been derived analytically, the sub-optimal solution of the cost function (24) is eliminated. Then the optimal solution of the cost function (24) drives the WMR to track the desired trajectory.

4 Stability analysis

In this section, the stability of the closed-loop error system (8) with the proposed MPC algorithm is given in the following.

Theorem 1: For the WMR system (1), consider the transformational system (16) and (17) and the cost function (24) with the soft constrains (25). A positive semi-definite matrix Q, positive definite matrix R, a predictive horizon N_p with $N_p\ge 1$ and a control horizon N_c with $1\le N_c\le N_p$ are chosen such that the optimal solution of the cost function (24)

$$[\Delta U^{*}(k)\varepsilon^{*}(k)]=[\Delta\tilde{u}^{*}(k)\,\Delta\tilde{u}^{*}(k+1)\cdots\Delta\tilde{u}^{*}(N_c-1)\,\varepsilon_1^{*}(k)\,\varepsilon_2^{*}(k)]^{\mathrm{T}} \tag{28}$$

holds. Let the optimal cost function $J^*(k)$ as a Lyapunov function $V^*(k)$ at time instant k. If the conclusion $V^*(k+1) \leq V^*(k)$ satisfies at time instant $k+1$, then the optimal solution (28) guarantees nominal stable of system (8).

Proof: Note that controller (9) is a combination of the feedforward controller and the feedback controller. The feedforward controller is obtained according to the reference trajectory. Hence, the nominal stable of system (8) is dependent on the feedback controller. In solution (28) of the cost function (24) with softening constrains (25), let $\Delta\tilde{u}^*(k+i|k)$ and $\varepsilon^*(k)$ be the optimal feedback control input increment and the optimal relaxing factor, respectively. Then $\tilde{u}^*(k+i|k)$ is the optimal feedback control input corresponding to the optimal feedback control input increment $\Delta\tilde{u}^*(k+i|k)$. The optimal cost function $J^*(k)$ is denoted as a Lyapunov function $V^*(k)$. One has that

$$\begin{aligned} V^*(k) &= \min\ J(k) \\ &= \min\left\{\sum_{i=1}^{N_p} \| \eta(k) - \eta_r(k) \|_Q^2 \right. \\ &\quad \left. + \sum_{i=0}^{N_c-1} \left[\| \Delta u(k) \|_R^2 + \| \epsilon(k) \|_\rho^2 \right] \right\} \end{aligned} \tag{29}$$

Obviously, the optimal function (29) satisfies $V^*(0) = 0$ for $k = 0$ and $V^*(k) > 0$ for arbitrary $k \neq 0$. For system (1) with external disturbances, the optimal control input increments $\Delta\tilde{u}(k+1+i|k+1)$ and relaxing factors $\varepsilon(k+1)$ are denoted as

$$\begin{aligned} \Delta\tilde{u}(k+1+i|k+1) &= [\Delta\tilde{u}(k+1|k+1), \Delta\tilde{u}(k+2|k+1), \\ &\quad \ldots, \Delta\tilde{u}(k+N_c|k+1)] \\ &= [\Delta\tilde{u}^*(k+1|k), \Delta\tilde{u}^*(k+2|k), \\ &\quad \ldots, \Delta\tilde{u}^*(k+N_c|k)] \end{aligned} \tag{30}$$

$$\varepsilon(k+1) = \varepsilon^*(k) \tag{31}$$

The feedback control input is shown as

$$\begin{aligned} \tilde{u}(k+1+i|k+1) &= [\tilde{u}(k+1|k+1), \tilde{u}(k+2|k+1), \\ &\quad \ldots, \tilde{u}(k+N_c|k+1)] \\ &= \tilde{u}^*(k+1|k), \tilde{u}^*(k+2|k), \\ &\quad \ldots, \tilde{u}^*(k+N_c|k)] \end{aligned} \tag{32}$$

It is easy to verify that (30)–(32) are a group of feasible solutions for the optimal question (24). The control increment $\Delta\tilde{u}(k+1+i|k+1)$ and the feedback controller $\tilde{u}(k+1+i|k+1)$ are belong to the constraint sets $\Omega_{\Delta u}$ and Ω_u.

According to (30)–(32), the relation between $J(k+1)$ and $V^*(k)$ is shown as follows: (see equation below) Furthermore, function $J(k+1)$ is not less than $V^*(k+1)$ due to optimality of the cost function (24). One has that

$$\begin{aligned} V^*(k+1) \leq J(k+1) \leq V^*(k) - & \| \eta^*(k) - \eta_r(k) \|_Q^2 \\ & - \| \Delta u^*(k) \|_R^2 - \| \epsilon^*(k) \|_\rho^2 \end{aligned}$$

and further

$$V^*(k+1) \leq V^*(k)$$

It is shown that the nominal stability of the closed-loop error system (8) is shown. □

Remark 3: Note that the bounded disturbances $d(k)$ have been considered in the cost function (24). Therefore, the proposed control sequences (28) have great robustness. Moreover, the Lyapunov function (29) satisfies $V^*(0) = 0$ with $k = 0$ and $V^*(k) > 0$ with arbitrary $k \neq 0$. And the Lyapunov function (29) is monotone decreasing, i.e. $V^*(k+1) \leq V^*(k)$ holds along the reference trajectory. Thus, the closed-loop error system (8) is nominally stability.

5 Simulation results

In this section, a double lane-changing trajectory [38] test is proposed to test the performance of trajectory tracking. In addition, a comparative simulation with the robust tracking controller in [10] is carried out to verify the effectiveness and robustness. The structure parameters of the WMR are given in Table 1.

5.1 Double lane-change trajectory test

The double lane-changing trajectory is defined as follows:

$$\begin{aligned} y_r(x(t)) &= \frac{4.05}{2}(1 + \tanh(z_1(t))) - \frac{5.7}{2}(1 + \tanh(z_2(t))) \\ \theta_r(x(t)) &= \arctan\left(4.05\left(\frac{1}{\cosh(z_1(t))}\right)^2\left(\frac{1.2}{25}\right)\right. \\ &\quad \left. -5.7\left(\frac{1}{\cosh(z_2(t))}\right)^2\left(\frac{1.2}{21.95}\right)\right) \end{aligned}$$

$$\begin{aligned} J(k+1) &= \sum_{i=1}^{N_p} \| \eta(k+1+i|k+1) - \eta_r(k+1+i|k+1) \|_Q^2 \\ &\quad + \sum_{i=0}^{N_c-1} \left[\| \Delta u(k+1+i|k+1) \|_R^2 \right. \\ &\quad \left. + \| \epsilon(k+1+i|k+1) \|_\rho^2 \right] \\ &= \sum_{i=2}^{N_p} \| \eta^*(k+i|k) - \eta_r(k+i|k) \|_Q^2 \\ &\quad + \sum_{i=1}^{N_c-1} \left[\| \Delta u^*(k+i|k) \|_R^2 + \| \epsilon^*(k+i|k) \|_\rho^2 \right] \\ &= \sum_{i=1}^{N_p} \| \eta^*(k+i|k) - \eta_r(k+i|k) \|_Q^2 \\ &\quad + \sum_{i=0}^{N_c-1} \left[\| \Delta u^*(k+i|k) \|_R^2 + \| \epsilon^*(k+i|k) \|_\rho^2 \right] \\ &\quad - \| \eta(k|k) - \eta_r(k|k) \|_Q^2 - \| \Delta u(k|k) \|_R^2 - \| \epsilon(k|k) \|_\rho^2 \\ &= V^*(k) - \| \eta(k|k) - \eta_r(k|k) \|_Q^2 - \| \Delta u(k|k) \|_R^2 \\ &\quad - \| \epsilon(k|k) \|_\rho^2 \end{aligned}$$

Table 1 Parameters of the WMR

Parameters	
$\tilde{u}_{\max} = [0.2\ \pi/3]^{\mathrm{T}}$	$\tilde{u}_{\min} = -\tilde{u}_{\max}$
$\Delta\tilde{u}_{\max} = [0.02\ \pi/30]^{\mathrm{T}}$	$\Delta\tilde{u}_{\min} = -\Delta u_{\max}$
$m = 10\,\mathrm{kg}$	$L = 0.22\,\mathrm{m}$
$r = 0.05\,\mathrm{m}$	

Table 2 Parameters of the proposed controller

Parameters	
$v_{1\max} = \mathrm{diag}\{0.1\ 0.1\}$	$v_{1\min} = -v_{1\max}$
$v_{2\max} = \mathrm{diag}\{0.01\ 0.01\}$	$v_{2\min} = -v_{2\max}$
$\rho = \mathrm{diag}\{5\ 5\}$	
$d_{\max} = \mathrm{diag}\{0.005\ 0.005\}$	$d_{\min} = -d_{\max}$
$h = 0.5$	$A_r = 0_{n\times n}$
$Q = 0.1I_{n\times n}$	$R = 5I_{m\times m}$
$N_p = 4$	$N_c = 3$

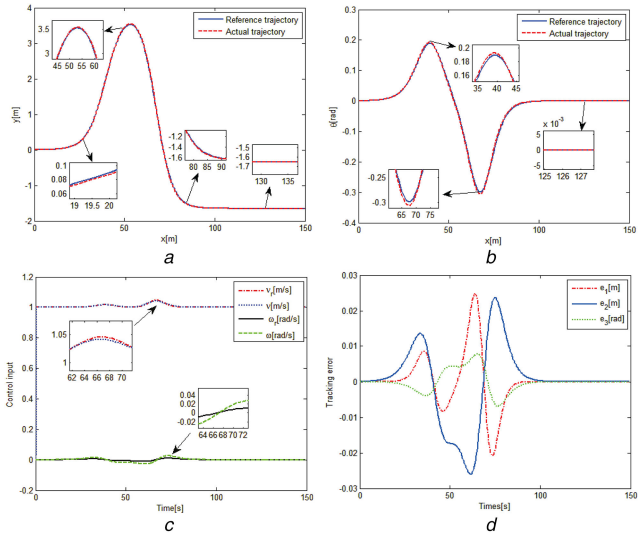

Fig. 4 *Performance of tracking a double lane-change trajectory based on MPC*

(a) Trajectory tacking of $y(x)$, ***(b)*** Trajectory tacking of $\theta(x)$, ***(c)*** Control input, ***(d)*** Trajectory tacking errors

Table 3 Parameters of the two controllers

Parameters	
Proposed controller	Robust controller in [10]
$Q = \mathrm{diag}\{10\ 10\ 0.05\}$	$k_o = 1.4$
$R = 0.1I_{m\times m}$	$k_t = 4$
$N_p = 4$	$k_{th} = 5$
$N_c = 3$	$k_f = 15$
$A_r = 0.95_{n\times n}$	

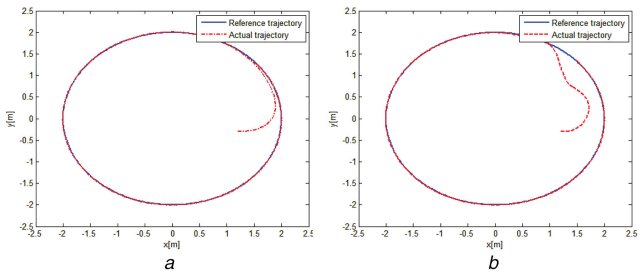

Fig. 5 *Trajectory tracking of WMR*

(a) Trajectory tracking for MPC, ***(b)*** Trajectory tracking in [10]

where $z_1(t) = (2.4/25)(x(t) - 27.19) - 1.2$ and $z_2(t) = (2.4/21.95)(x(t) - 56.46) - 1.2$. It is obvious that both $y_r(x(t))$ and $\theta_r(x(t))$ are the non-linear functions on $x(t)$. In the double lane-changing trajectory test, the relevant parameters about the proposed controller are shown in Table 2.

The simulation results are shown in Fig. 4.

The trajectory tracking results of the double lane-changing trajectory are shown in Figs. 4*a* and *b*. The control inputs are presented in Fig. 4*c*. The trajectory tracking errors are shown in Fig. 4*d*. From the results in Fig. 4, the tacking performance of the proposed controller (27) is better and the WMR tracks the designed trajectory and the reference control inputs. From Fig. 4*d*, the trajectory tacking errors exist when the WMR turns orientation. However, the errors are tiny within the range of acceptable performance quality.

5.2 Comparative simulations

A comparative simulation with the robust tracking controller in [10] is shown in the following section. The WMR is controlled to follow a circle trajectory which is given as follows:

$$x_r(t) = 2\sin(0.2t), \quad y_r(t) = 2\cos(0.2t) \tag{33}$$

where $t \in [0, 35]$ s. In the comparative simulation, the initial conditions of WMR are the same, $[x(0)\ y(0)\ \theta(0)]^{\mathrm{T}} = [1.2, -0.3, 0]^{\mathrm{T}}$, which starts with initial state errors for the desired trajectory (33). The sampling interval is set as $h = 0.1$ s. In the proposed MPC, the adjustable coefficients have large change range in simulation. One group of parameters for the proposed controller and the proper parameters on the robust controller in [10] are shown in Table 3. The comparative simulation results are shown in Figs. 5–7. Trajectory tracking of the WMR is shown in Fig. 5.

It is shown that the WMR actuated by both the proposed controller (27) and robust tracking controller in [10] tracks the circle trajectory despite there exist the initial state errors. However, the tracking performance using the proposed controller (27) is smoother than that in [10]. The trajectory tracking errors are shown in Fig. 6.

The tracking errors using controller (27) asymptotically converge to zero nearly more quickly than the robust controller in [10]. The control input quantities of tracking the circle are presented in Fig. 7.

The linear velocity and angular velocity finally stabilise exactly to 0.4 m/s and 0.2 rad/s, respectively. Furthermore, the proposed controller (27) is smooth and is limited in the range of the physical constraint of the WMR while the robust controller in [10] did not consider the constraints.

In addition, the performance qualities under the proposed controller and the robust controller in [10] are shown in Figs. 8 and 9 when the WMR starts with different initial conditions.

The controller coefficients are the same as Table 3. The initial conditions are $[x(0)\ y(0)\ \theta(0)]^{\mathrm{T}} = [2\ 0\ \pi/2]^{\mathrm{T}}$, $[x(0)\ y(0)\ \theta(0)]^{\mathrm{T}} = [2.5\ 0\ 3\pi/2]^{\mathrm{T}}$ and $[x(0)\ y(0)\ \theta(0)]^{\mathrm{T}} = [0\ -2.5\ 0]^{\mathrm{T}}$.

The performance quality under the proposed controller is better than the robust controller in [10] without changing the coefficients.

Finally, a comparative simulation with the receding horizon controller in [23] is designed to show the performance quality of the proposed controller. The simulation results under the receding horizon controller are found in [23] and the simulation results under the proposed controller are shown in Fig. 10.

Note that the conditions are same as the ones of circle test in [23]. In Fig. 10*a*, the WMR tracks the circle trajectory well under the proposed controller. In Fig. 10*b*, the linear velocity and angular velocity finally stabilise to 0.4 m/s and 0.5 rad/s, respectively. In Fig. 10*c*, it is shown that the tracking errors converge more quickly under the proposed controller in this paper than the robust controller in [23]. That is, the WMR tracks the reference trajectory at $t \simeq 6.5$ s and $t \simeq 12$ s under the proposed controller in this paper and the receding horizon controller in [23], respectively. It is also

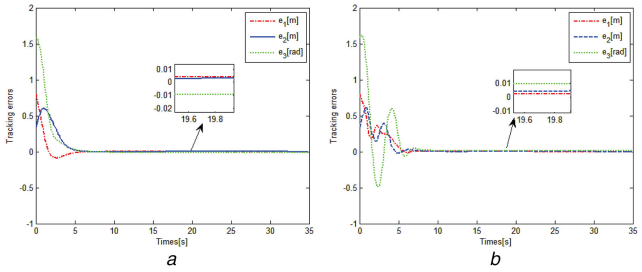

Fig. 6 *Trajectory tracking errors*
(a) Tracking errors for MPC, ***(b)*** Tracking errors in [10]

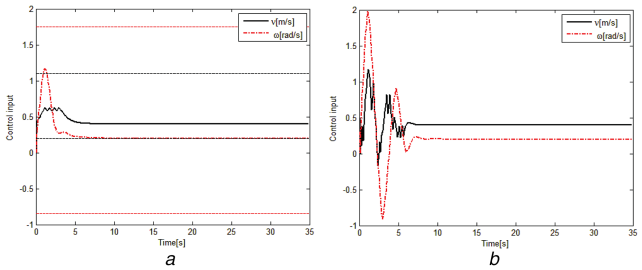

Fig. 7 *Control input of WMR*
(a) Control input for MPC, ***(b)*** Control input in [10]

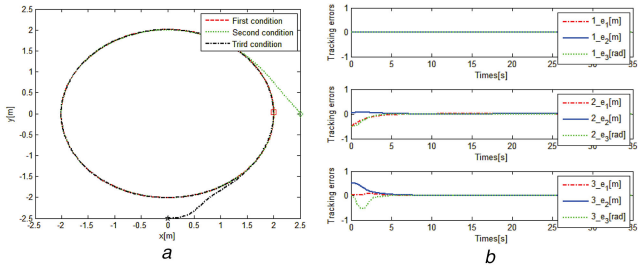

Fig. 8 *Different initial state based on MPC*
(a) Trajectory tracking for MPC, ***(b)*** Tracking errors for MPC

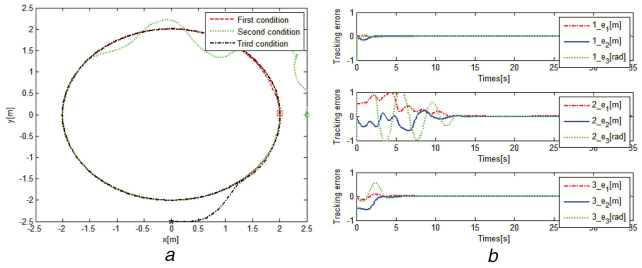

Fig. 9 *Different initial states in [10]*
(a) Trajectory tracking in [10], ***(b)*** Tracking errors in [10]

shown in Fig. 10*c* that the steady-state errors are smaller in this paper than the ones in [23]. Therefore, all of the simulation results verify the robustness and effectiveness of the proposed control strategy.

Remark 4: In [37], the control horizon N_c is set as time that the output response reaches 60% of the process steady state. For example, the WMR tracks the reference trajectory at $t \simeq 5$ s in Fig. 6*a*, then the control horizon N_c is set as 3. As the predicted horizon N_p is not less than the control horizon N_c. Much computation time has to take with N_p increasing, then N_p is set as 4. In this case, it is shown from $Q = \text{diag}\{10\,10\,0.05\}$ that the control for the orientation error has the lowest sensitivity. Similarly, the weighting matrix is set as $R = 0.1I_{m\times m}$.

Remark 5: Both external disturbance and the high-order linearisation term are considered for a kinematic model of the WMR in this paper. However, neither external disturbances nor the high-order linearisation term is contained in [23]. Furthermore, control increment constraints and a relaxing factor are designed in this paper to avoid control jump and infeasible solutions, respectively. However, the conditions on control jump and infeasible solutions are not considered in [23]. Moreover, it is also shown in Fig. 10 that the simulation results under the proposed controller in this paper are better than the ones under the receding horizon controller in [23].

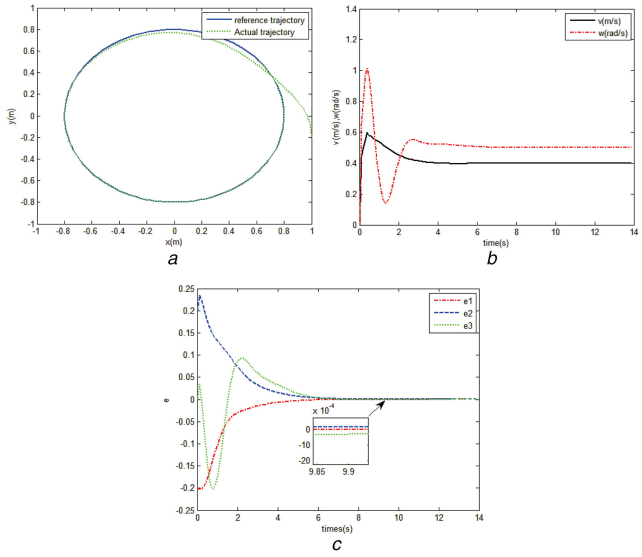

Fig. 10 *Circle tracking for MPC*
(a) Trajectory tracking for MPC, ***(b)*** Control input for MPC, ***(c)*** Tracking errors for MPC

6 Conclusion

A control strategy based on MPC with softening constraints has been presented for the WMR to track the reference trajectories. In the WMR model, some external disturbances and control input increment constraints have been considered. Both robustness and smoothness of the proposed controller are ensured. Theoretical analysis shows that the stability is achieved by the proposed controller of the WMR. Finally, two simulation results show the effectiveness and smoothness of the proposed control scheme.

7 References

[1] Hu, J.S., Wang, J.J., Ho, D.M.: 'Design of sensing system and anticipative behavior for human following of mobile robots', *IEEE Trans. Ind. Electron.*, 2014, **61**, pp. 1916–1927

[2] Cui, R., Li, Y., Yan, W.: 'Mutual information-based multi-AUV path planning for scalar field sampling using multidimensional RRT', *IEEE Trans. Syst. Man Cybern. Syst.*, 2016, **46**, pp. 993–1004

[3] Brockett, R.: *Differential geometric control theory*, Birkhauser Press, Basel, 1983

[4] Jiang, Z., Nijmeijer, H.: 'Tracking control of mobile robots: a case study in backstepping', *Automatica*, 1997, **33**, pp. 1393–1399

[5] Ge, S.S., Wang, Z., Lee, T.H.: 'Adaptive stabilization of uncertain nonholonomic systems by state and output feedback', *Automatica*, 2003, **39**, pp. 1451–1460

[6] Yang, S.X., Zhu, A., Yuan, G., *et al.*: 'A bioinspired neurodynamics-based approach to tracking control of mobile robots', *IEEE Trans. Ind. Electron.*, 2012, **59**, pp. 3211–3220

[7] Michalek, M., Kozlowski, K.: 'Vector-field-orientation feedback control method for a differentially driven vehicle', *IEEE Trans. Control Syst. Technol.*, 2009, **18**, pp. 45–65

[8] Chwa, D.: 'Sliding-mode tracking control of nonholonomic wheeled mobile robots in polar coordinates', *IEEE Trans. Control Syst. Technol.*, 2004, **12**, pp. 637–644

[9] Park, B.S., Park, J.B., Choi, Y.H.: 'Robust adaptive formation control and collision avoidance for electrically driven nonholonomic mobile robots', *IET Control Theory Appl.*, 2011, **5**, pp. 514–522

[10] Yang, H., Fan, X., Xia, Y., *et al.*: 'Robust tracking control for wheeled mobile robot based on extended state observer', *Adv. Robot.*, 2015, **30**, pp. 1–11

[11] Xin, L., Wang, Q., She, J., Li, Y.: 'Robust adaptive tracking control of wheeled mobile robot', *Robot. Auton. Syst.*, 2016, **78**, pp. 36–48

[12] Hwang, C.L., Wu, H.M.: 'Trajectory tracking of a mobile robot with frictions and uncertainties using hierarchical sliding-mode under-actuated control', *IET Control Theory Appl.*, 2013, **7**, pp. 952–965

[13] Shen, Z., Ma, Y., Song, Y.: 'Robust adaptive fault-tolerant control of mobile robots with varying center of mass', *IEEE Trans. Ind. Electron.*, 2017 DOI: 10.1109/TIE.2017.2740845
[14] Chen, M.: 'Disturbance attenuation tracking control for wheeled mobile robots with skidding and slipping', *IEEE Trans. Ind. Electron.*, 2017, **64**, pp. 3359–3368
[15] Ouadah, N., Ourak, L., Boudjema, F.: 'Car-like mobile robot oriented positioning by fuzzy controllers', *Int. J. Adv. Robot. Syst.*, 2008, **5**, pp. 249–256
[16] Rossomando, F.G., Soria, C., Carelli, R.: 'Neural network-based compensation control of mobile robots with partially known structure', *IET Control Theory Appl.*, 2012, **6**, pp. 1851–1860
[17] Yuan, Y., Sun, F., Liu, H.: 'Resilient control of cyber-physical systems against intelligent attacker: a hierarchal Stackelberg game approach', *Int. J. Syst. Sci.*, 2016, **47**, pp. 2067–2077
[18] Yuan, Y., Yuan, H., Guo, L.*, et al.*: 'Resilient control of networked control system under DoS attacks: a unified game approach', *IEEE Trans. Ind. Inf.*, 2016, **12**, pp. 1786–1794
[19] Song, Y., Huang, X., Wen, C.: 'Tracking control for a class of unknown nonsquare MIMO nonaffine systems: a deep-rooted information based robust adaptive approach', *IEEE Trans. Autom. Control*, 2016, **61**, pp. 3227–3233
[20] Jerez, J.L., Ling, K.V., Constantinides, G.A.*, et al.*: 'Model predictive control for deeply pipelined field-programmable gate array implementation: algorithms and circuitry', *IET Control Theory Appl.*, 2012, **6**, pp. 1029–1041
[21] Lu, C.H., Tsai, C.C.: 'Adaptive predictive control with recurrent neural network for industrial processes: an application to temperature control of a variable-frequency oil-cooling machine', *IEEE Trans. Ind. Electron.*, 2008, **55**, pp. 1366–1375
[22] Lee, S.M., Myung, H.: 'Receding horizon particle swarm optimisation-based formation control with collision avoidance for non-holonomic mobile robots', *IET Control Theory Appl.*, 2015, **9**, pp. 2075–2083
[23] Gu, D., Hu, H.: 'Receding horizon tracking control of wheeled mobile robots', *IEEE Trans. Control Syst. Technol.*, 2006, **14**, pp. 743–749
[24] Gu, D., Yang, E.: 'A suboptimal model predictive formation control'. Proc. IEEE/RSJ Int. Conf. Intelligent Robots and Systems, 2005, pp. 1295–1300
[25] Nascimentoa, T.P., Moreira, A.P., Conceição, A.G.S.: 'Multi-robot nonlinear model predictive formation control: moving target and target absence', *Robot. Auton. Syst.*, 2013, **61**, pp. 1502–1515
[26] Gao, Y., Lee, C.G., Chong, K.T.: 'Receding horizon tracking control for wheeled mobile robots with time-delay', *J. Mech. Sci. Technol.*, 2008, **22**, pp. 2403–2416
[27] Barreto, J.C.L., Conceição, A.G.S., Dórea, C.E.T.: 'Design and implementation of model-predictive control with friction compensation on an omnidirectional mobile robot', *IEEE/ASME Trans. Mechatronics*, 2014, **19**, pp. 467–476
[28] Kühne, F., Fetter, W., João, L.*, et al.*: 'Model predictive control of a mobile robot using linearization'. Proc. Mechatronics and Robotics, 2004
[29] Zhang, D., Wang, Q.G., Srinivasan, D.*, et al.*: 'Asynchronous state estimation for switched complex networks with communication constraints', *IEEE Trans. Neural Netw. Learn. Syst.*, 2017, **99**, pp. 1–15
[30] Yuan, Y., Yuan, H., Wang, Z.*, et al.*: 'Optimal control for networked control systems with disturbances: a delta operator approach', *IET Control Theory Appl.*, 2017, **11**, pp. 1325–1332
[31] Pepy, R., Lambert, A., Mounier, H.: 'Reducing navigation errors by planning with realistic vehicle model'. Intelligent Vehicles Symp., 2006, pp. 300–307
[32] Guechi, E.H., Lauber, J., Dambrine, M.*, et al.*: 'Output feedback controller design of a unicycle-type mobile robot with delayed measurements', *IET Control Theory Appl.*, 2012, **6**, pp. 726–733
[33] Lin, C.F., Ulsoy, A.G., LeBlanc, D.J.: 'Vehicle dynamics and external disturbance estimation for vehicle path prediction', *IEEE Trans. Control Syst. Technol.*, 2000, **8**, pp. 508–518
[34] Zhang, D., Shi, P., Wang, Q.G.*, et al.*: 'Analysis and synthesis of networked control systems: a survey of recent advances and challenges', *ISA Trans.*, 2017, **66**, pp. 376–392
[35] Li, Z., Yang, C., Su, C.Y.*, et al.*: 'Vision-based model predictive control for steering of a nonholonomic mobile robot', *IEEE Trans. Control Syst. Technol.*, 2016, **24**, pp. 553–564
[36] De Oliveira, N.M.C., Biegler, L.T.: 'Constraint handing and stability properties of model-predictive control', *AIChE J.*, 1994, **40**, pp. 1138–1155
[37] Garriga, J.L, Soroush, M.: 'Model predictive control tuning methods: a review', *Ind. Eng. Chem. Res.*, 2010, **49**, pp. 3505–3515
[38] Falcone, P., Tseng, H.E., Borrelli, F.*, et al.*: 'MPC-based yaw and lateral stabilisation via active front steering and braking', *Veh. Syst. Dyn.*, 2008, **46**, pp. 611–628